IJMT. Vol. 23, Iss. 1, 202. (117-134)

International Journal of Maritime Technology

Journal homepage: ijmt.ir

Numerical Investigation of GFRP-Reinforced Underwater Steel Pipes Under Blast Loading

Mohammad Esmaeilzadeh[1],Mehdi Behdarvandi Askar[2*]

[1] Graduated of Offshore Structures, Department of Offshore Structures, Faculty of Marine Engineering, Khorramshahr University of Marine Science and Technology, *m.esmaeilzadeh@gmail.com*

[2] **Associate professor, Department of marine structures, khorramshahr university of marine science and technology, sazehenteghal@yahoo.com*

ARTICLE INFO

Article History:
Received: 27 Jul 2026
Last modification: 3 Oct 2026
Accepted:
Available online:

Article type:
Research Paper

Keywords:
Ti Steel,pipes,
underwater explosions,
GFRP
mes New Roman 9
Times New Roman 9
Up to 5 Phrases

ABSTRACT

The analysis of the behavior of submerged steel pipes subjected to underwater explosions is of great importance, as these pipes are used in many offshore foundations, piers, and marine structures. In this study, the behavior of submerged steel pipes under underwater explosions is investigated using numerical modeling in ABAQUS software. First, the validity of the model was verified by comparing the results with a reference paper. Then, by simulating three explosive scenarios with different TNT masses at a distance of 5 meters from the pipe, the results showed that with increasing TNT mass, the kinetic energy and strain of the pipe increase .Furthermore, four different pipe strengthening methods using GFRP sheets were investigated. The results showed that continuous use of GFRP is the most effective method for reducing stress, deformation and pipe damage under underwater explosions. This method can reduce local pipe deformation by up to 52%. Additionally, the use of closely spaced GFRP rings can also be effective in reducing pipe stress and deformation to some extent .The findings of this study showed that underwater explosions cause less damage to the pipe than explosions in air due to the damping of blast waves in water. This study also assists designers and engineers in the design and strengthening of submerged pipes in underwater environments. However, experimental tests are recommended for more accurate research and to investigate the effects of other factors such as type of bed soil and water temperature.

ISSN: 2645-8136

DOI:

Copyright: © 202 by the authors. Submitted for possible open access publication under the terms and conditions of the Creative Commons Attribution (CC BY) license [https://creativecommons.org/licenses/by/4.0/]

[Downloaded from ijmt.ir on 2026-10-24]

1. Introduction

In today's rapidly evolving technological landscape, the maintenance and operation of industrial infrastructure have become paramount. Consequently, the safety and blast resistance of metallic structures have emerged as significant challenges. Underwater explosions constitute a physical phenomenon occurring within water or other fluids, generating shock waves and pressure pulses. While commonly associated with aquatic environments or near-surface occurrences, these explosions can manifest in various fluid mediums. Such events are typically attributed to factors like elevated pressure, intense heat, mechanical shock, or a combination thereof. Underwater explosions have long captivated researchers and engineers due to their complex nature, making them a focal point for studies aimed at informing design decisions related to structural engineering, maritime safety, and other aquatic applications. Moreover, research into the blast resistance of underwater structures and pipelines has gained prominence. In this context, steel pipelines, employed for subsea transportation of various substances, play a pivotal role. Given the potential blast hazards prevalent in the oil and gas industries and other related sectors, the reinforcement of these pipelines using advanced materials such as glass fiber has become increasingly imperative. The application of Fiber Reinforced Polymers (FRPs) for the rehabilitation and strengthening of steel structures remains an active area of research [1-7] Geers and Hunter[8] developed a wave-integrated model for moderately deep underwater explosion (UNDEX) bubbles, coupling the shock and oscillation phases. A hyperacoustic formulation predicted far-field pressure from bubble acceleration, and spherical bubble motion equations were validated with experiments. Results showed improved accuracy over earlier models in predicting bubble-surface displacement histories. Monteiro et al [9] investigated the dynamic collapse of submerged cylindrical shells under impulsive pressure loads using a combined experimental and numerical approach. They subjected aluminum tubes with a diameter-to-thickness ratio of 32.3 to underwater explosions at varying distances. The experiments captured the dynamic pressure and collapse behavior, while finite element models were developed to simulate the entire process. The study provided valuable insights into the response of cylindrical shells to impulsive pressure loadings. Dereli et al. [10]address limitations of traditional piping blast analysis by proposing a more efficient MDOF FEA method using Abaqus/Explicit. Their approach considers non-linearities and utilizes a scripting tool to convert existing data for faster analysis. This method reduces the need for additional pipe supports compared to traditional methods. Emamzadeh et al.[11] investigated the nonlinear dynamic response of a fixed offshore platform subjected to underwater explosions (UNDEX) at varying distances. Their model considers the effects of blast bubble fluctuations and water interaction on the platform's natural frequencies. The study revealed that near-field explosions cause localized damage, while medium to far-field events induce significant base shear due to a wider area being exposed to the blast pressure. Their findings highlight the importance of UNDEX risk assessment and potential member strengthening for offshore platform safety. George et al.[12] investigated the effectiveness of underwater composite repair with fibre reinforced polymers (FRP) for corroded offshore structural members. Their experimental study on steel tubular members subjected to concentric and eccentric axial loads revealed that underwater repairs can achieve similar ultimate strength as conventional in-air repairs. A finite element model accurately predicted the experimental behaviour, suggesting the viability of underwater FRP repairs for offshore applications. However, further research is needed to assess the long-term performance and cyclic behaviour of these repairs (Engineering Structures, Experimental and numerical investigation of underwater composite repair with fibre reinforced polymers in corroded tubular offshore structural members under concentric and eccentric axial loads). The study by Hsu et al. [13]investigated the use of Glass Fibre Reinforced Polymer (GFRP) laminates for ship structures subjected to underwater shock loading. They compared the material properties obtained through static and dynamic testing, highlighting the influence of high strain rates on stress-strain behaviour. Finite element simulations using ABAQUS software demonstrated that dynamic material properties resulted in a more pronounced strain response compared to static properties. Their findings suggest the importance of considering dynamic material behaviour when designing FRP composite ship structures for underwater shock resistance. Liu et al[14] . simulate subsea pipelines under underwater explosions for UXO removal using a coupled Eulerian-Lagrangian method. This method considers the seabed and captures its influence on the pipeline response at different explosion offsets. Their work offers a valuable tool for improving safety assessments during UXO removal operations .Kristoffersen et al.[15] used live C-4 to investigate how blast loading affects concrete pipes Mimicking potential threats to submerged floating tunnels, they detonated explosives inside and outside unreinforced pipes.

[Downloaded from ijmt.ir on 2026-10-24]

High-speed cameras and sensors captured the response. Notably, a larger C-4 charge was needed to breach the pipe when detonated externally, showcasing the concrete's confinement effect. Lam et al [16]. focus on laminated pipelines, their research offers valuable insights into the response of underwater structures to shock loading. Their study employs a fluid-structure interaction model to analyze a simply supported underwater pipeline subjected to underwater explosion. The pipe's response is characterized as local deformation, with the radial direction experiencing the most significant displacement due to its weaker strength compared to the circumferential and longitudinal directions. The study also explores the influence of parameters like charge weight, standoff distance, and pipe length. Liang and Tai [17] employed a combined finite element and asymptotic approach to simulate the shock response of a patrol boat under underwater explosions. This method incorporated transient dynamics, geometric nonlinearities, material plasticity, and fluid-structure interaction. The study identified plastic zone formation and hull deformation patterns, aiding in designing warships with improved resistance to underwater shock damage. Liu et al.[18] introduced a continuous Eulerian finite element approach to simulate underwater explosions. This method overcomes limitations of prior methods by treating the entire explosion (shockwave and bubble motion) as a single process, particularly important near walls. Their model captures the full explosion sequence and highlights the value of continuous simulation for accurate bubble motion near walls. Peng et al[19]. present a numerical approach for simulating structural damage caused by near-field underwater explosions. Their method couples Smoothed Particle Hydrodynamics (SPH) for the fluid with Reproducing Kernel Particle Method (RKPM) for the structure. A key aspect of their work is the contact detection algorithm for the RKPM shell formulation, crucial for handling large deformations during underwater explosions. They employ a normal-flux method, treating the structure as a moving boundary for the fluid and fluid pressure as the load on the structure. This research contributes to the FSLAB software for structural damage analysis under underwater explosions. Qu et al.[20] use a 3D finite element model to simulate the impact of non-spherical charges on near-field underwater explosion pressure distribution .Their work highlights the influence of shape and orientation on pressure, finding significant deviations from spherical charges. This emphasizes the need to consider these factors in underwater explosion design, and they even propose a reference formula for non-spherical charge peak pressure. Razic and Miralem [21] investigated the underwater explosion effects of a 60mm mortar bomb on a cylindrical concrete structure . Their experiment employed a concrete pipe filled with water and submerged the mortar bomb directly in the water pointing towards the bottom . They documented the fragmentation of the bomb and the effects on the concrete structure, including the distance at which fragments posed no threat . This research provides valuable data for understanding underwater explosions and their impact on submerged concrete structures. In a review by Tran et al.[22]. composite materials are gaining traction in shipbuilding due to their weight and radar signature advantages . However, these structures are susceptible to complex damage under underwater explosions (UNDEX). The review explores research conducted over the past 20 years on the response of composite structures to UNDEX . It covers experimental programs, modeling approaches, post-explosion analysis techniques, and analytical methods . The authors delve into the stages of an UNDEX event, including shock wave formation, attenuation, cavitation, and fluid-structure interaction . They summarize state-of-the-art experimental programs that investigate these phenomena, including the influence of low temperatures and cavitation . The review also discusses various modeling approaches, including hydrocodes and their limitations due to simplifications and reliance on experimental data . Finally, Tran et al.[22] data-driven modeling techniques using artificial neural networks as potential tools to enhance predictive capabilities. Li et al. [23]employed the boundary integral method to model large-scale airgun-bubble dynamics, incorporating non-spherical features and air release processes. Their simulations reproduced experimental pressure waveforms and revealed that port opening time and Froude number significantly influence bubble collapse intensity and pressure peak, offering insights for optimizing airgun designs. Zhang et al.[24] employed a unified bubble dynamics equation to investigate bubble behavior under hybrid-boundary and multi-bubble conditions. By modeling complex boundary interactions and validating with spark bubble experiments, they showed that cavitation bubble clusters can produce pressure peaks nearly twice as high as single bubbles, emphasizing their destructive potential. Liang et al.[25] conducted a comprehensive study on spherical bubble oscillations and shock wave emission from laser-induced cavitation in water. Using advanced imaging and simulations, they quantified bubble wall velocities, shock front dynamics, and energy partitioning. Results highlighted that most energy radiated acoustically and rebound pressure peaked at 13.5 GPa. Zhang et al.[26] proposed a novel theoretical model for compressible bubble dynamics

[Downloaded from ijmt.ir on 2026-10-24]

that incorporates phase transition, migration, and ambient flow effects. The model, extensible and physically consistent, accurately predicts bubble behavior near boundaries and in free fields. Results showed vapor content and Mach number significantly influence energy loss and pressure radiation. Preso et al.[27] investigated vapor compression and energy dissipation during laser-induced bubble collapse in aqueous ammonia. Results showed that higher vapor pressures reduce collapse intensity and energy loss, promote spherical symmetry, and suppress interface instabilities. Shock wave emission was found not to be the dominant dissipation mechanism at collapse.

2. Objective

This research aims to employ finite element analysis to investigate the dynamic response of submerged pipelines subjected to underwater explosions. The study will focus on evaluating the effectiveness of GFRP reinforcement in mitigating damage and improving the structural integrity of pipelines. By simulating underwater explosions of varying magnitudes and analyzing the resulting stress distributions, deformations, and failure modes, this research will provide valuable insights into the design and optimization of blast-resistant pipeline systems. Specifically, the study will compare the performance of pipelines reinforced with different GFRP configurations, with the goal of identifying the most effective reinforcement strategy.

3. Theoretical Background for Numerical Analysis

3.1. Shock Wave Pressure Modeling

When an explosive charge detonates in an underwater environment, the initial and most intense loading mechanism is the propagation of a high-pressure shock wave through the surrounding water medium. This transient pressure pulse is responsible for inducing immediate structural deformation and potential damage to nearby submerged structures such as steel pipelines. The time history of this pressure load can be effectively modeled using the Friedlander equation, which captures the exponential decay of pressure after reaching its peak value:

$$P(t) = P_0 \cdot e^{-t}\left(1 - \frac{t}{T}\right) \quad (1)$$

In this formulation, P_0 represents the peak overpressure generated by the explosion, while θ accounts for the rate at which the pressure decays over time due to energy dissipation and geometric spreading. The parameter T defines the duration of the positive phase of the pressure pulse, during which the pressure remains above ambient levels.

This model has been widely adopted in numerical simulations involving underwater explosions due to its simplicity and reasonable accuracy in capturing the early-time behavior of the shock wave [28]. In addition to the Friedlander equation, the Hopkinson–Cranz scaling law is often employed to estimate the peak pressure at a given distance from the source based on the scaled depth of burst:

$$Z = \frac{R}{W^{1/3}} \quad (3)$$

Here, Z denotes the scaled distance in meters per kilogram to the power of one-third, R is the physical distance from the center of the explosion to the target structure, and W refers to the equivalent mass of TNT used in the simulation. This scaling law enables efficient modeling of various explosion scenarios without recalibrating the entire model, allowing engineers to extrapolate experimental data obtained from standard charges to real-world conditions

Furthermore, the Kingery–Bulmash empirical equations have been extensively utilized to predict both the peak pressure and impulse of the shock wave, providing a more detailed description of the pressure-time curve[29]. These formulations are particularly valuable when precise estimation of structural response under impulsive loading is required, and they form the basis for many modern finite element simulations involving underwater blast events.

3.2. Bubble Pulse Loading

Following the initial shock wave, the formation and subsequent pulsation of the gas bubble generated by the explosive charge constitute a secondary but equally important source of loading. Unlike the shock wave, which acts almost instantaneously, the bubble pulse develops over a longer time period and contributes significantly to the residual damage sustained by submerged structures, especially during the collapse phase where jet formation and localized high-pressure impacts may occur.

The dynamics of the expanding and collapsing bubble can be accurately simulated using the Keller–Miksis equation, which extends the classical Rayleigh–Plesset equation to account for compressibility effects in the surrounding fluid:

$$R\ddot{R} + \frac{3}{2}\dot{R}^2 = c\dot{R} + \frac{1}{\rho}\left[P_g - P_\infty(t) - \frac{2\sigma}{R} - \frac{4\mu\dot{R}}{R}\right] \quad (4)$$

[Downloaded from ijmt.ir on 2026-10-24]

In this expression, R represents the instantaneous radius of the bubble, while $\dot{R}$ and $\ddot{R}$ denote its first and second time derivatives, respectively. The density of the surrounding fluid, typically water, is represented by ρ and plays a key role in determining the inertial forces acting on the bubble. The internal pressure within the bubble, P_g, is counteracted by the ambient hydrostatic pressure $P\infty(t)$, which varies with depth and time. Additional factors influencing the bubble dynamics include surface tension σ which stabilizes small bubbles, and fluid viscosity μ which affects the dissipation of energy during bubble oscillations. Finally, the speed of sound in the fluid, denoted by c, is included to account for wave propagation effects in the surrounding medium[30].

To further characterize the behavior of the bubble, additional parameters such as the bubble period and maximum radius are defined:

$$T_b = K_T \cdot \left(\frac{W^{1/3}}{(P_\infty)^{1/6}}\right), R_{max} = K_R \cdot W^{1/3} \quad (5)$$

These relationships allow for the prediction of bubble characteristics without requiring full dynamic simulation, making them valuable tools in preliminary design and risk assessment studies. Moreover, the Taylor bubble velocity potential method can be applied to estimate the momentum transfer from the bubble to nearby structures, offering a simplified way to evaluate the resulting impulse and structural displacement caused by the bubble motion[31] .

3.3. Bubble Migration

In the study of underwater explosion bubbles, bubble migration plays a significant role in determining the overall system dynamics, energy distribution, and pressure wave propagation within the surrounding fluid. Recent theoretical advancements, such as those proposed by Zhang et al., have introduced a unified framework for simulating compressible bubble dynamics. These models go beyond traditional oscillation and collapse processes by incorporating phase change effects, fluid compressibility, and thermal boundary layer interactions at the gas–liquid interface.

The derived bubble migration equation within this framework accounts for both inertial forces arising from the surrounding flow field and resistive forces due to pressure gradients and viscous effects. Notably, phase-change processes particularly evaporation and condensation appear as additional source terms in the momentum equations and significantly influence the bubble's translational velocity. These effects are more pronounced in high-pressure bubbles, where vapor mass transfer leads to changes in internal gas composition and alters the intensity of bubble collapse.Moreover, studies have shown that bubble migration is not solely governed by local pressure gradients but is also indirectly affected by fluid compressibility through the coupling of volumetric acceleration and translational motion. In compressible flows, acoustic waves generated during bubble collapse can create asymmetric pressure fields around the bubble, leading to directional movement and increased energy dissipation into the surrounding medium.

Compared to earlier models, these updated formulations offer improved accuracy in predicting bubble trajectories near boundaries and in multi-bubble scenarios. They also show good agreement with experimental observations of bubble jet formation, toroidal deformation, and inter-bubble interactions.Although the current numerical model employs simplifying assumptions such as spherical symmetry and constant vapor content future improvements could benefit from incorporating advanced theories that include compressibility-modified added mass coefficients and phase-change-coupled momentum equations. Such enhancements would increase the accuracy of numerical predictions, particularly in estimating bubble-induced loads and assessing cavitation damage potential in complex underwater environments.

4. Numerical study (FEM-based)

4.1. Verification

To validate the numerical model, given the dynamic nature of the problem and the focus on underwater explosions, two separate verification studies were conducted in this research.First, the benchmark study of Jen et al. [22] was selected. This study investigated the response of an optimized ring-stiffened hull for small underwater vehicles subjected to underwater explosions. The objective was to minimize hull weight while enhancing its capacity to resist hydrostatic pressure, underwater blast loads, and other environmental conditions. The authors employed a robust optimization method to design the pressure hull of an unmanned underwater vehicle, which consisted of a ring-stiffened cylindrical shell with hemispherical end caps. A finite element model (FEM) was then developed to analyze the transient dynamic response of the hull under shock wave pressure from an underwater explosion. The simulation method employed was

[Downloaded from ijmt.ir on 2026-10-24]

UNDEX, which is also used in the present study and implemented using the Abaqus software.

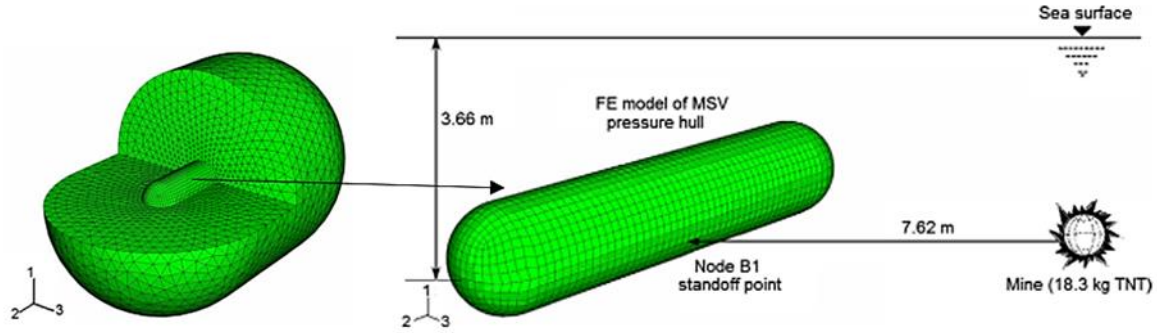

Figure 1. Warfare scenarios of MSV [32]

As illustrated in Figure 1, this model served as a simplified representation of submerged structures exposed to underwater blast scenarios. The comparison of results indicated that the Abaqus finite element software, along with the UNDEX blast simulation approach, was capable of predicting the dynamic response with acceptable accuracy. Figure 2(a) presents the deformation of the hull at initial and final monitored states, showing a maximum discrepancy of approximately 6%. Additionally, Figure 2(b) displays the plastic strain contours, further confirming the overall validity of the numerical approach. While the model provides a close approximation, the observed 6% deviation highlights the inherent complexity in accurately simulating underwater explosion events

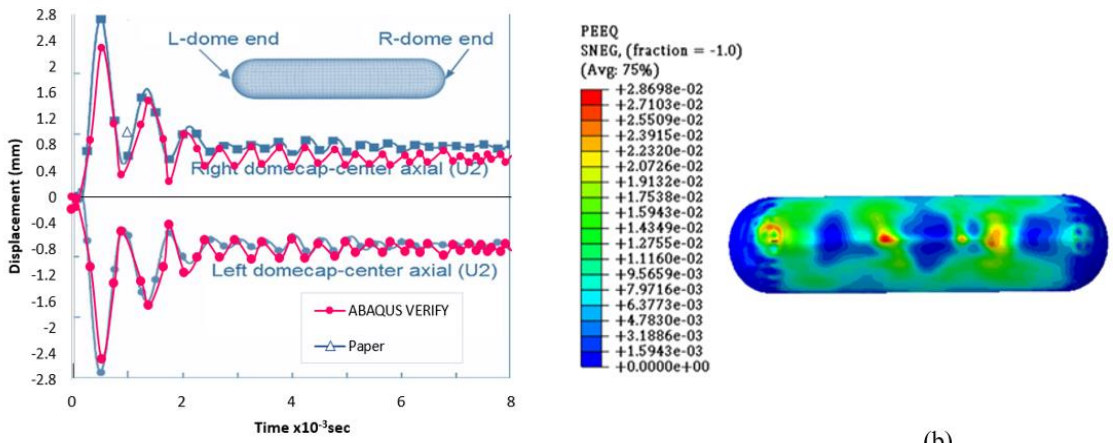

(a) (b)

Figure 2. (a) Comparison of Predicted and Simulated Float Deformation. (b) Plastic Strain Distribution in Underwater Float

Second, a laboratory-based experimental model was utilized to further validate the reliability of the numerical simulation[33]. In this phase, a hull structure subjected to underwater explosion loading (UNDEX) was modeled using Abaqus and the results were compared with experimental data reported in the literature. The primary validation metric was the strain measured at the midpoint of the hull. The comparison revealed a maximum discrepancy of approximately 7% between the numerical and experimental results, indicating that the finite element model is capable of accurately capturing the mechanical response of hull structures under underwater blast conditions. As illustrated in Figure 3, the comparison encompasses both strain and displacement data, along with contour plots depicting stress distribution across the hull. It is important to highlight that experimental investigations on underwater explosion phenomena are relatively scarce, primarily due to the inherent challenges, high costs, and safety considerations involved in such testing. Therefore, the close agreement observed in this two-tier verification approachcomprising both numerical-to-numerical and numerical-to-experimental comparisonsoffers

[Downloaded from ijmt.ir on 2026-10-24]

strong validation for the accuracy and applicability of the proposed simulation framework.

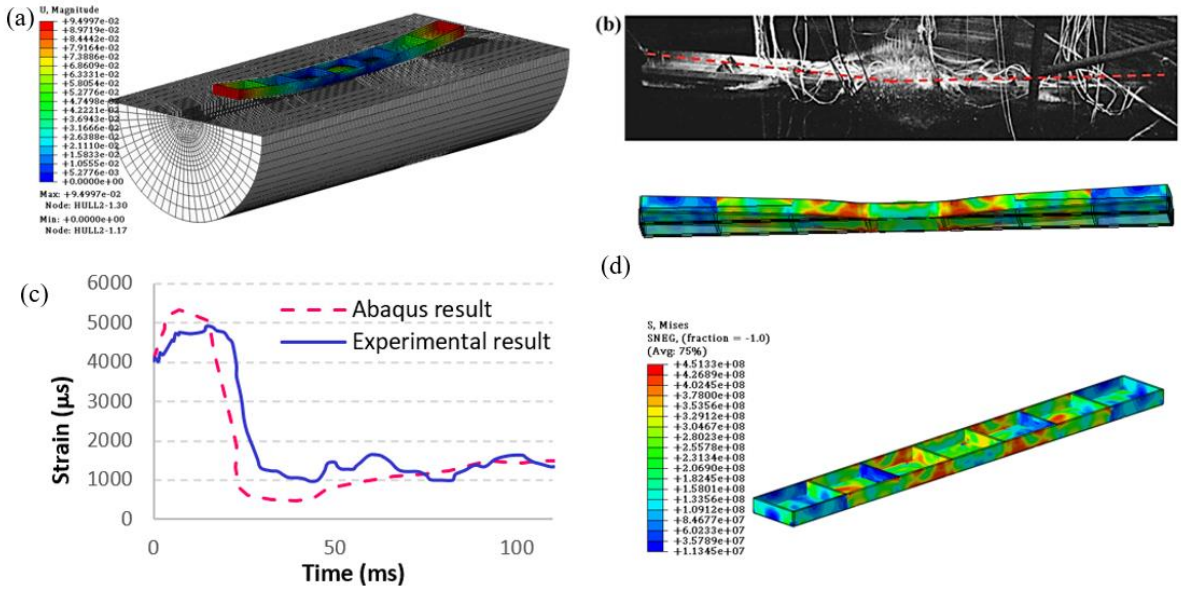

Figure 3. (a) Deformation contour of the hull (b) Experimental deformation of the specimen (c) Strain comparison at the mid-point (d) Stress contours in the hull

4.2. Simulation pipeline under water

A submerged pipe with a diameter of 96 cm, a thickness of 28 mm, and a length of 10 meters was modeled. The pipe was submerged in a water-filled domain, with its centerline located 5 meters below the free surface. The explosive charge was also positioned at a depth of 5 meters and was varied in terms of TNT mass. A schematic illustrating the pipe and the surrounding fluid domain is provided in the Figure 4.

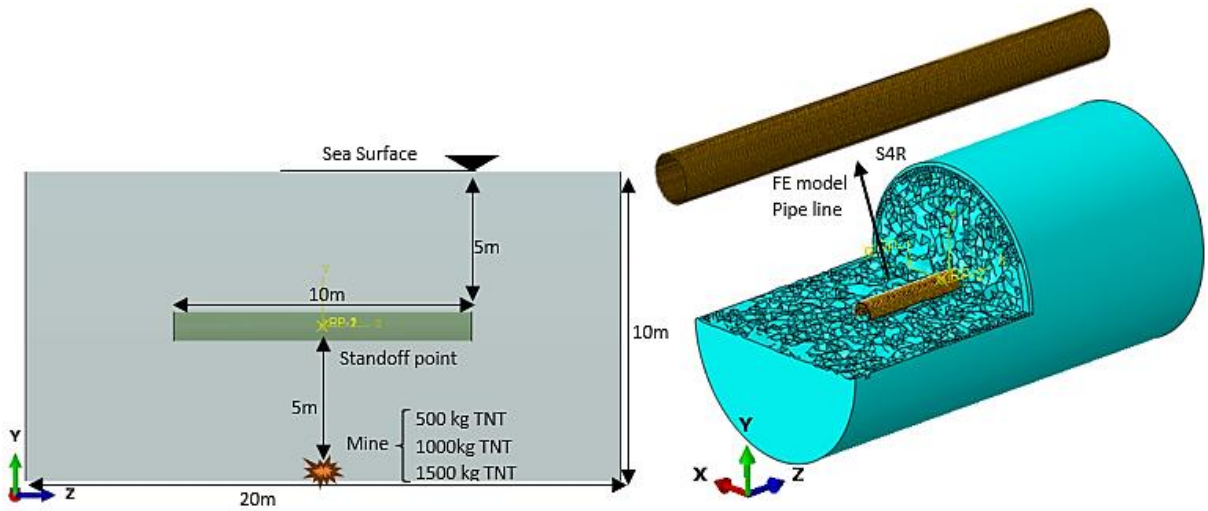

Figure 4. Dimensional details and 3D FEM modeling of a pipe in a fluid environment

The S4R four-node shell element with six degrees of freedom per node (three translations and three rotations) was employed to model the pipeline shell. The element connectivity is such that each shell normal is oriented towards the external fluid. The external fluid domain was discretized using four-node acoustic tetrahedral elements of type AC3D4.

[Downloaded from ijmt.ir on 2026-10-24]

4.3. Material models

The accurate representation of material behavior under dynamic loading conditions is crucial for the reliable prediction of structural response. In this study, the pipeline material was selected as API 5L X70 steel. Due to the extreme loading rates associated with underwater explosions, the material's response deviates significantly from its quasi-static behavior. To account for this, the Cowper-Symonds model was employed to incorporate strain rate effects into the material constitutive model. The Cowper-Symonds model introduces a dynamic hardening factor (DHF) to scale the static yield stress to obtain the dynamic yield stress. This relationship is expressed in Equation (1). Furthermore, to capture the reduction in ductility under dynamic loading, the failure strain was modified using the Jones' model, as presented in Equation (2). The model parameters C and p, which govern the strain rate sensitivity of the material, were assumed to be 4000 s^-1 and 5, respectively, as recommended for offshore steels. By incorporating these material models, the analysis aimed to provide a more realistic representation of the pipeline's behavior under the impulsive loading conditions induced by underwater explosions.

$$\boldsymbol{\sigma_y^d = \sigma_y^s \left[1 + \left(\frac{\dot{\varepsilon}}{C}\right)^1 / p\right]} \quad (6)$$

$$\boldsymbol{\varepsilon_f^d = \xi \cdot \varepsilon_f^s \left[1 + \left(\frac{\dot{\varepsilon}^1}{C} / p\right)\right]^{-1}} \quad (7)$$

σ_y^d: Dynamic yield stress (resistance under high strain rate loading)

σ_y^s: Static yield stress (resistance under low strain rate loading)

$\dot{\varepsilon}$: Strain rate (rate of deformation)

C and p : Material constants (affecting strain rate sensitivity)

ε_f^d: Dynamic failure strain (maximum strain before failure under high strain rate)

ε_f^s: Static failure strain (maximum strain before failure under low strain rate)

ξ : Ratio of total energies to rupture (dynamic vs. static uniaxial loading)

To accurately represent water properties in the model, an equation of state (EOS) was employed. A constant density of 1000 kg/m³ and a viscosity of 0.001 Pa·s were assumed for water. The curve coefficients necessary for the EOS were obtained from the attached figure. The GFRP material was modeled as a laminate, consistent with the findings of Lee et al.[34] The Hashin failure criterion was adopted to characterize the failure behavior of the GFRP composite. Performance parameters of glass fiber-reinforced polymer laminate

Table 1 Performance parameters of glass fiber-reinforced polymer laminate

Constitutive parameters	E_{11} (GPa)	E_{22} (GPa)	E_{33} (GPa)	G_{12} (GPa)	G_{13} (GPa)	G_{23} (GPa)	μ_{12}	μ_{13}	μ_{23}
Value	48.6	8.5	8.5	3.5	3.5	3	0.33	0.33	0.38
Strength parameters	X_T (MPa)	X_c (MPa)	Y_T (MPa)	Y_c (MPa)	S_{12} (MPa)	S_{13} (MPa)	S_{23} (MPa)		
Value	1900	550	43	90	93	93	50		

To ensure the accuracy of the numerical simulation of the submerged steel pipe reinforced with GFRP under underwater blast loading, a mesh convergence analysis was conducted. In this study, various mesh sizes 4 cm, 8 cm, 14 cm, 20 cm, and 26 cm were evaluated (as illustrated in Figure 5). The key output variable was the strain at the reference point located at the mid-span of the pipe . The results indicated that reducing the element size from 26 cm to 14 cm led to less than 5% variation in stress and displacement. Further refinement to 8 cm and 4 cm resulted in variations of less than 1.5% , indicating

[Downloaded from ijmt.ir on 2026-10-24]

minimal improvement in accuracy. However, the significant increase in computational time for finer meshes (4 cm and 8 cm) highlighted the importance of selecting an appropriate mesh size.Therefore, to achieve a reasonable balance between accuracy and computational efficiency, the 4 cm mesh size was selected as the optimal mesh. This ensured sufficient accuracy in predicting structural behavior without imposing excessive computational cost.

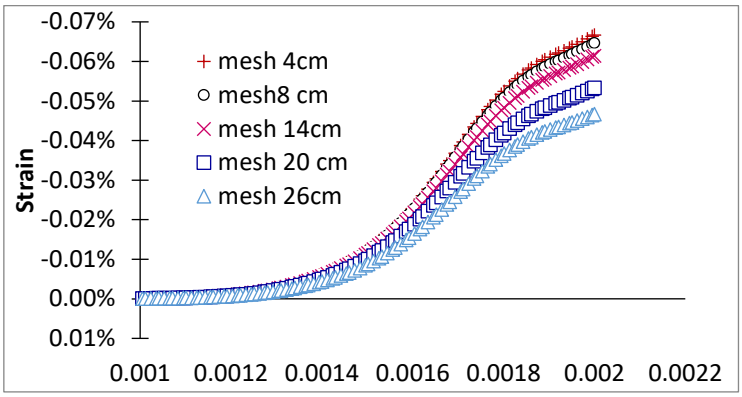

Figure 5. Strain results with respect to mesh size variation

5. Numerical results and discussions

Three explosion scenarios were simulated at a standoff distance of 5 meters, each with a different TNT charge mass. Subsequent analysis and reinforcement design focused on the most critical scenario, characterized by the highest TNT charge. The explosion duration was assumed to be 2 milliseconds.Fig. depicts the evolution of the explosion bubble within the fluid as it propagates towards the pipe. The kinetic and strain energy responses of the pipe under various explosive loading conditions are presented in the following figures.

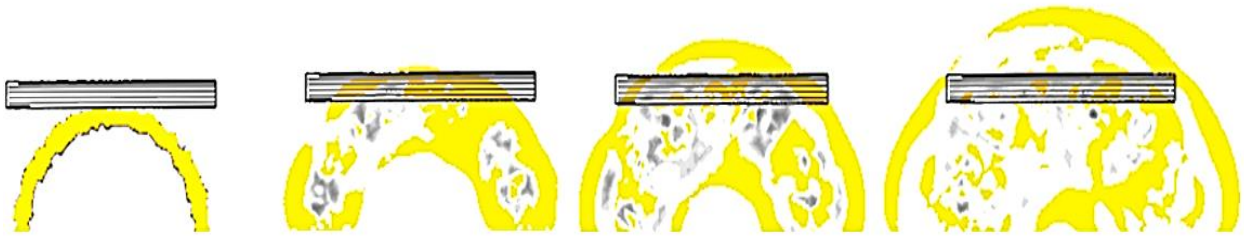

Figure 6. visualization of the growing explosion bubble in the UNDEX simulation.

The analysis of explosion scenarios involving 500 kg, 1000 kg, and 1500 kg TNT charges detonated 5 meters underwater revealed that the strain energy of the pipe exhibited less than a 5% difference within the initial phase, up to 0.001 seconds post-detonation. The peak difference in strain energy was observed at approximately 0.0016 seconds post-detonation. Regarding the kinetic energy extracted from the software (represented by ALLKE), it was found that among the analyzed scenarios, at 0.0004 seconds post-detonation, the difference in kinetic energy was less than 5%. The peak difference in kinetic energy between the 1000 kg and 1500 kg TNT scenarios occurred at 0.0008 seconds post-detonation. As a heuristic example, based on the obtained numerical results, a kinetic energy of 1,200,000 units could create a crater approximately 1 meter in diameter and 600 cm deep in soil. It is important to note that underwater explosions, due to the damping effect of water on shock waves, can significantly attenuate and disperse the blast wave. This results in reduced pressure and stress on the pipe during underwater explosions. Additionally, the density of water is significantly higher than that of air, increasing the water's resistance to deformation and the propagation of shock waves. Furthermore, water acts as a natural coolant, preventing excessive heating of the pipe during the explosion. Excessive heating can weaken and embrittle the pipe

[Downloaded from ijmt.ir on 2026-10-24]

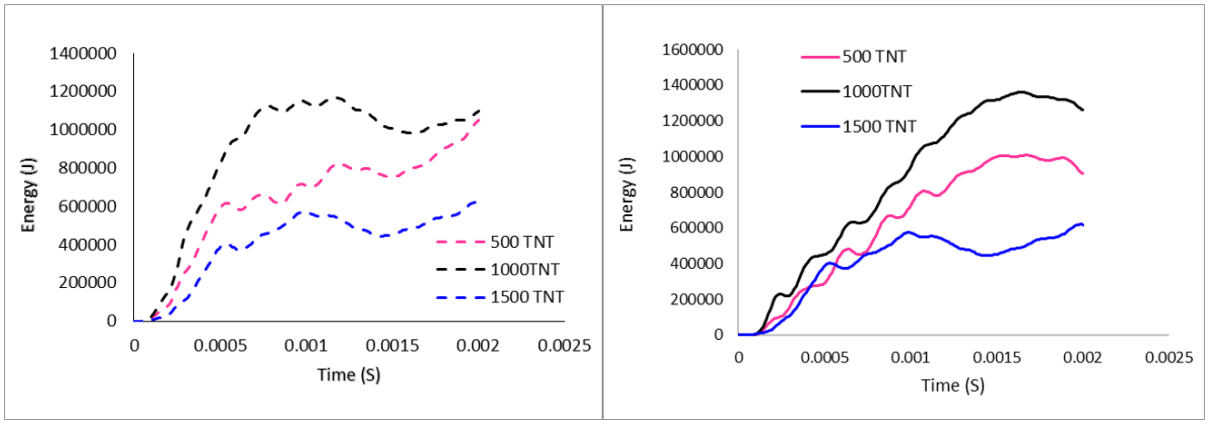

Figure 7. Strain and Kinetic Energy Response of Pipe to Underwater Explosions

graphical results clearly illustrate that the distribution of stress and the extent of damage varied considerably among the different explosion scenarios. presents a visualization of the von Mises stress and plastic strain distribution in the pipe, indicating a growing level of damage

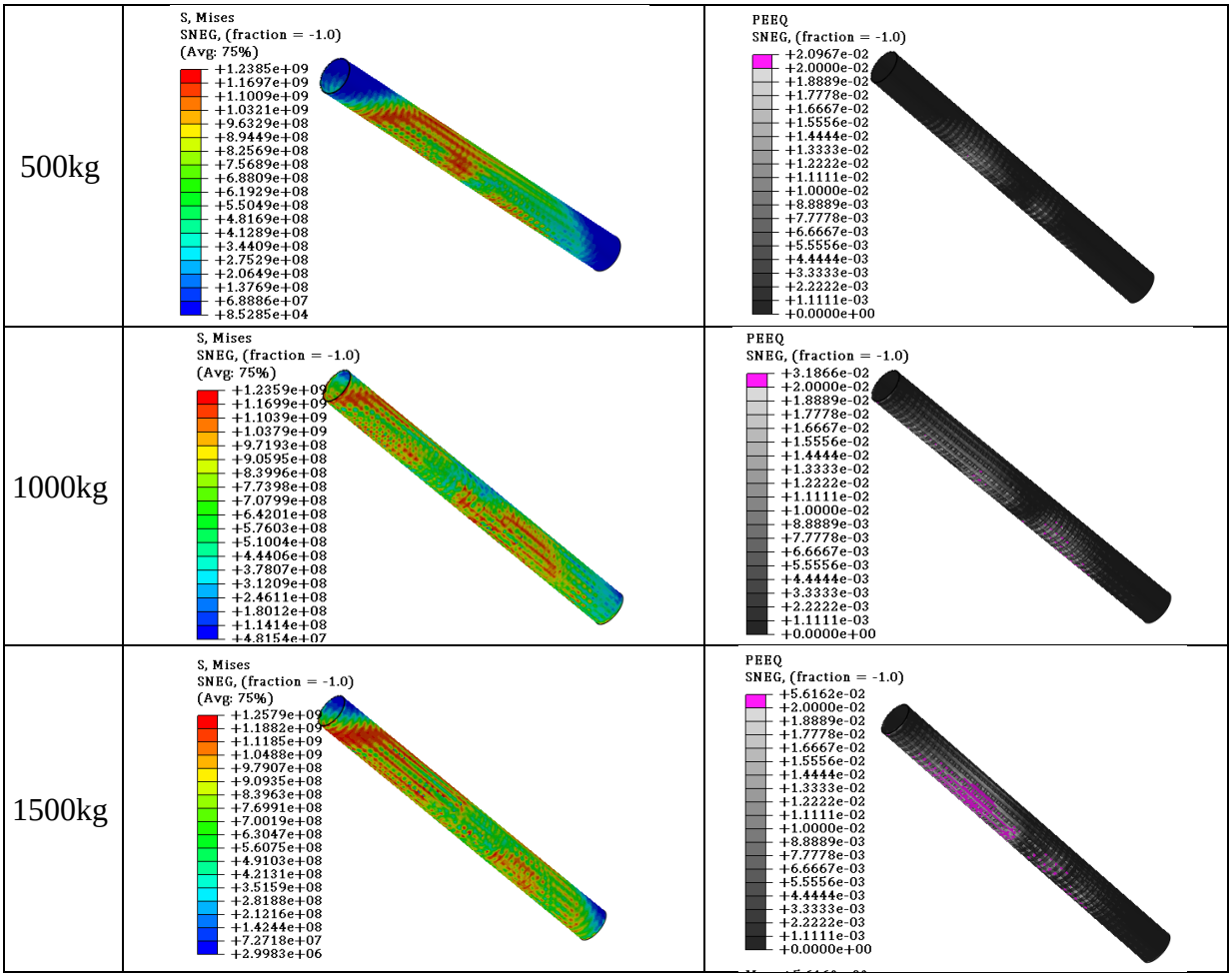

Figure8. Stress and strain distribution in different TNT scenarios

5.1. Structural behavior

To enhance the structural capacity, two layers of 3 mm thick FRP sheets were bonded to the structure in the second phase of the analysis. These sheets were orthogonally oriented and subjected to different reinforcement patterns. The schematic representation of the proposed reinforcement models is presented in theFig. .A parametric study was conducted to evaluate the performance of various FRP reinforcement configurations on submerged pipes under explosive loading. Five numerical models were developed for this purpose.

[Downloaded from ijmt.ir on 2026-10-24]

The baseline model, P0, represented an unreinforced pipe. To assess the influence of discrete reinforcement, models PG1 and PG2 were created, incorporating 50 cm and 20 cm wide FRP rings, respectively, spaced at intervals of 50 cm and 90 cm along the pipe's length. A continuous FRP spiral wrapping with a pitch of 500 cm and a width of 25 cm was employed in model PG3 to simulate a more uniform reinforcement distribution. Finally, model PG4 represented a pipe fully encased in FRP. By comparing the responses of these models, the optimal reinforcement configuration for mitigating the effects of underwater explosions can be determined.

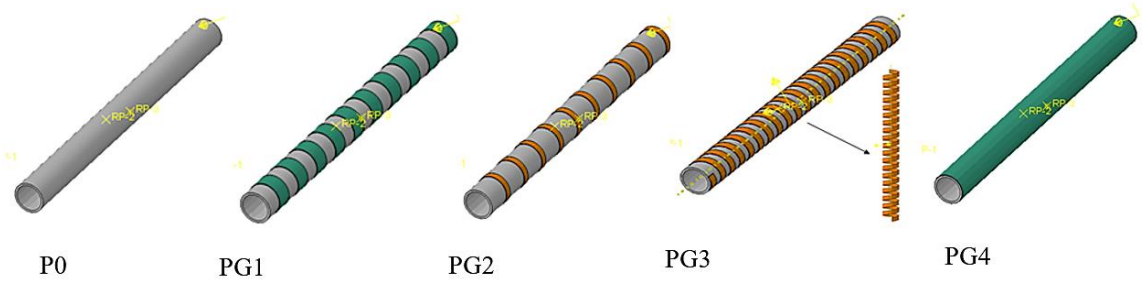

Figure 9. Different GFRP reinforcement configurations for pipes

A comparative analysis of the deformation behavior of the five pipe models subjected to underwater explosions revealed significant variations in their structural response. The unreinforced pipe, P0, exhibited the most severe deformation, reaching a maximum displacement of 76 mm, as depicted inFig. . This model demonstrated localized plastic strain, indicative of potential structural damage, particularly in the vicinity of the explosion. Models PG1 and PG2, reinforced with discrete FRP rings, showed a reduction in maximum deformation compared to P0. However, both models exhibited stress concentrations at the FRP-pipe interface, especially near the explosion zone. PG1, with larger and more widely spaced rings, experienced a maximum displacement of approximately 43 mm. PG2, with smaller and more closely spaced rings, demonstrated slightly better performance but still exhibited non-uniform deformation patterns, suggesting potential localized damage under more severe loading conditions. Model PG3, featuring a continuous FRP spiral wrapping, exhibited a substantial improvement in deformation behavior compared to the discretely reinforced models. The maximum displacement was reduced to 36 mm, and stress concentrations were significantly mitigated. The continuous reinforcement provided more uniform load distribution and enhanced the overall structural integrity of the pipe. Finally, model PG4, with a full FRP encasement, demonstrated the most robust performance. The maximum displacement was reduced to 35 mm, representing a 52% decrease compared to the unreinforced pipe. The uniform distribution of FRP around the pipe's circumference resulted in a more even stress distribution and minimal plastic deformation. While this model offered the most effective protection against explosive loading, the economic implications of full encasement should be carefully considered. In conclusion, the results of this study indicate that the use of FRP reinforcement can significantly improve the deformation behavior of submerged pipes subjected to underwater explosions. The continuous FRP wrapping (PG4) proved to be the most effective configuration, offering superior protection against explosive loading. However, the optimal reinforcement strategy will depend on various factors, including the severity of the expected explosion, the cost of materials and installation, and the specific requirements of the application.

[Downloaded from ijmt.ir on 2026-10-24]

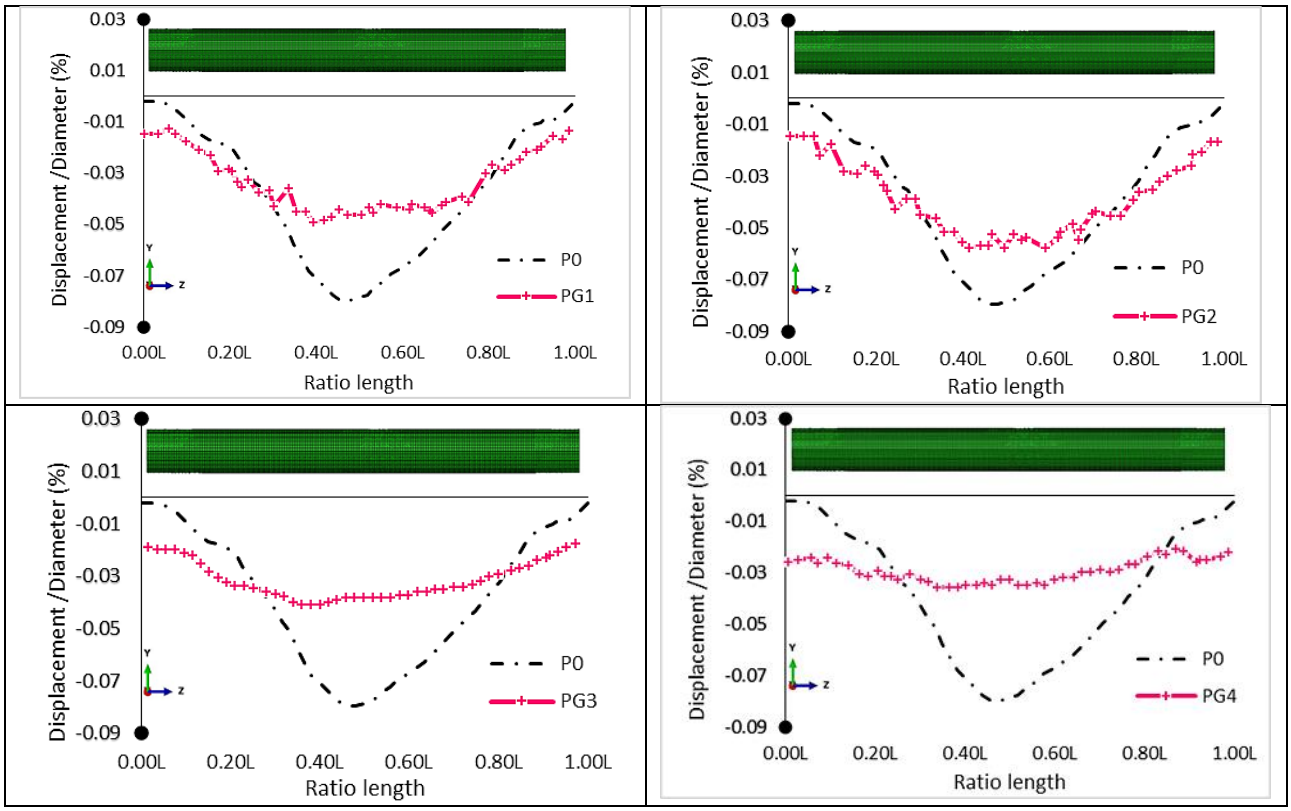

Figure 10. Displacement comparison between bare and reinforced pipes

5.2. Stress Distribution

The distribution of stress within each pipe model is illustrated in Figure 5. The results indicate that the unreinforced pipe (Model P0) experiences the highest stress concentration near the explosion site. This localized stress leads to extensive plastic strain, which is an indicator of potential local failure and the onset of structural damage.In Models PG1 and PG2, which are reinforced with discrete FRP rings, a significant reduction in the maximum stress values compared to Model P0 is observed. However, stress concentrations still persist at the corners of the rings and at the interface between the FRP and the steel. This phenomenon may initiate material debonding or localized failure under more severe loading conditions.Model PG3, which is strengthened with continuous helical FRP wrapping, exhibits a more uniform stress pattern compared to the discrete reinforcement models. This improved stress distribution reduces the likelihood of critical stress zones and enhances the overall structural performance of the pipe.Model PG4, fully encased in FRP, achieves the most favorable stress distribution. In this model, stress is well-distributed along the circumference of the pipe, and stress concentrations are minimized. The continuous FRP layer effectively transfers the load around the pipe, resulting in an improved elastic-plastic response. These results demonstrate that the use of continuous FRP reinforcement can significantly reduce the probability of stress-induced failures in submerged pipes subjected to explosive loading.

[Downloaded from ijmt.ir on 2026-10-24]

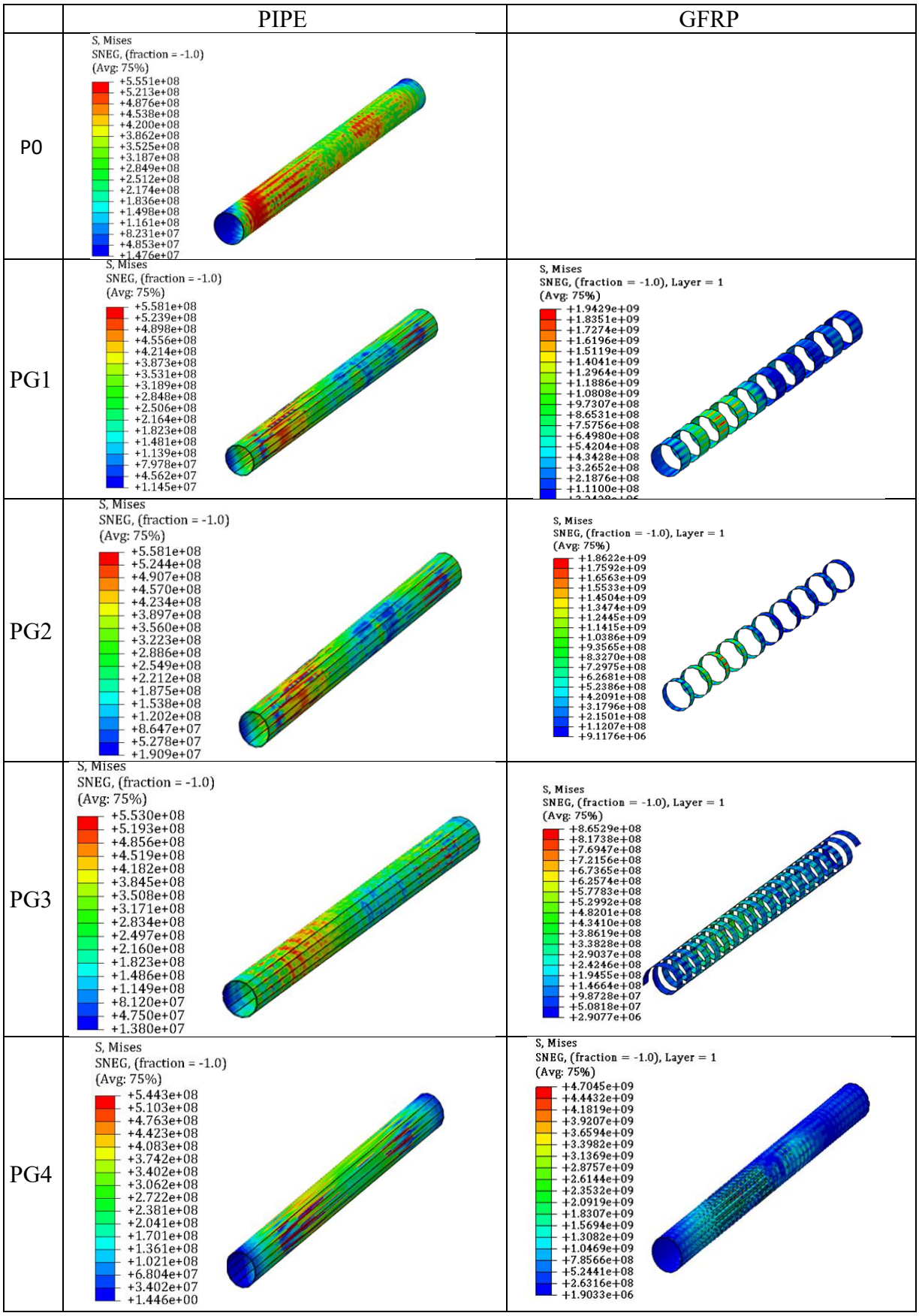

Figure 11. Stress distribution comparison in models with GFRP reinforcement

As shown in Figure 12(a), the variation of stress on the outer surface of the unreinforced pipe is presented schematically with exaggerated visualization. This diagram helps provide a physical understanding of how the explosion affects the pipe. Additionally, Figure 12(b) compares the maximum stress distribution among all models at the peak time

[Downloaded from ijmt.ir on 2026-10-24]

of the explosion. The results show that the difference in maximum stress between the unreinforced model (P0) and Model PG4 reaches up to 31%. This notable difference highlights the effectiveness of full GFRP wrapping in reducing structural stresses.

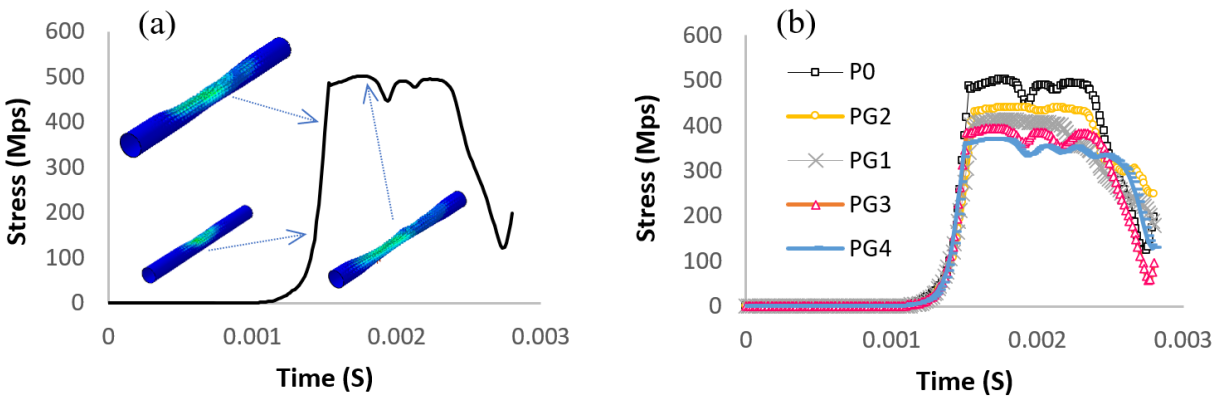

Figure 12. a. Schematic representation of stress variation on the outer surface of the unreinforced pipe (P0) under underwater blast loading (exaggerated visualization for clarity)

5.3. Plastic Strain

Figure illustrates the distribution of plastic strain within each pipe model following the explosive loading event. The unreinforced pipe, P0, exhibited the most extensive regions of plastic strain, indicating significant material damage. The concentration of plastic strain was particularly pronounced in the vicinity of the explosion, where the material exceeded its elastic limit. Models PG1 and PG2, reinforced with discrete FRP rings, showed a reduction in the overall extent of plastic strain compared to P0. However, localized plastic strains were still observed at the interface between the FRP rings and the pipe, suggesting potential debonding or failure in these regions under more severe loading conditions. Model PG3, with its continuous FRP spiral wrapping, demonstrated a significant reduction in plastic strain compared to the discretely reinforced models. The continuous reinforcement effectively distributed the load and limited the development of localized plastic zones. Model PG4, fully encased in FRP, exhibited the smallest extent of plastic strain, indicating that the complete encasement provided the most effective protection against plastic deformation. These findings highlight the importance of continuous reinforcement in mitigating plastic strain and enhancing the overall structural integrity of the pipe.

[Downloaded from ijmt.ir on 2026-10-24]

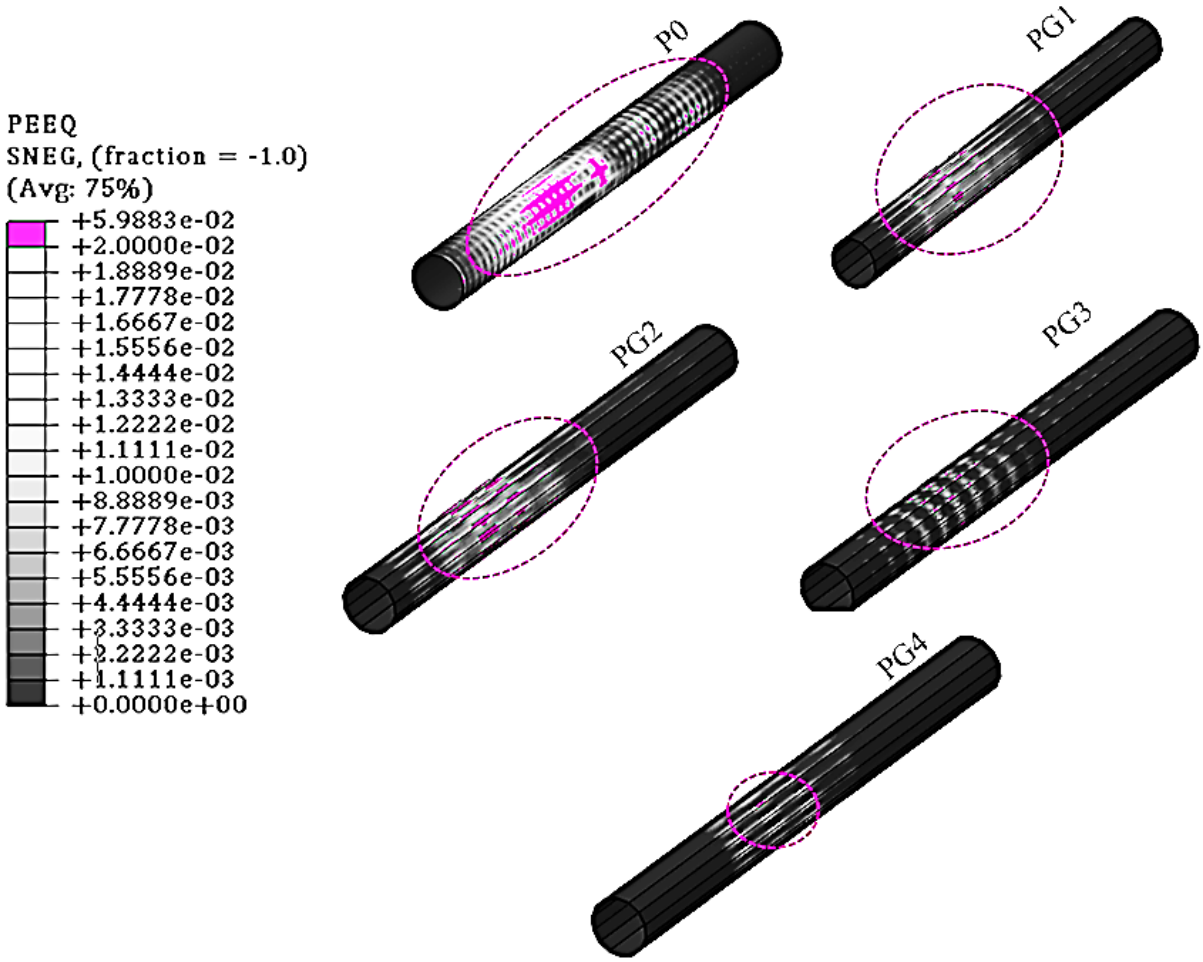

Figure 13.Comparison of plastic strain in models subjected to a 1500 kg TNT blast load

6. Conclusion

This study utilized finite element analysis to assess the effectiveness of various GFRP reinforcement configurations in enhancing the structural performance of submerged steel pipelines subjected to underwater blast loading. The numerical results clearly indicate that GFRP reinforcement significantly improves the resistance of pipelines against explosive loads, with continuous wrapping proving to be the most effective strategy. Compared to the unreinforced baseline model (P0), the fully wrapped configuration (PG4) reduced maximum local deformation by more than 50%, resulting in a more uniform stress distribution and minimal plastic strain.While localized reinforcement methods such as discrete FRP rings (PG1 and PG2) also contributed to structural improvement, they were less effective due to stress concentrations observed at the ring-pipe interfaces, which may lead to premature failure or debonding under severe loading conditions. Model PG3, featuring spiral wrapping, offered an intermediate solution with improved load distribution and moderate protection against structural damage.The findings of this research highlight the potential of continuous GFRP reinforcement as a reliable method for improving the blast resistance of underwater pipelines. This approach can be particularly beneficial in offshore environments where submerged pipelines are exposed to potential threats such as underwater mines, unexploded ordnances, or accidental explosions during marine operations.

7. References

1- Elchalakani, M., Karrech, A., Basarir, H., Zhao, X.-L., Fawzia, S., Hassanein, M. F. (2017). **Strengthening of mild steel struts using CFRP sheets subjected to uniform axial compression**. Thin-Walled Structures, 116, 96-112. https://doi.org/10.1016/j.tws.2017.03.013

2- Bambach, M. R., Elchalakani, M. (2007). **Plastic mechanism analysis of steel SHS strengthened with CFRP under large axial deformation**. Thin-Walled Structures, 45(2), 159-170. https://doi.org/10.1016/j.tws.2006.12.006

3- Elchalakani, M., Fernando, D. (2012). **Plastic mechanism analysis of unstiffened steel I-*

[Downloaded from ijmt.ir on 2026-10-24]

*section beams strengthened with CFRP under 3-point bending**. Thin-Walled Structures, 53, 58-71. https://doi.org/10.1016/j.tws.2011.12.013

4- Xiong, C., Shao, Y., Tong, L., Dai, K., Luo, Y. (2023). **Static strength of CFRP-strengthened preloaded circular concrete-filled steel tube stub columns, Part I: Experimental test**. Thin-Walled Structures, 184, 110546. https://doi.org/10.1016/j.tws.2022.110546

5- Alshamrani, S., Rasheed, H. A., Salahat, F. H., Borwankar, A., Divilbiss, N. (2024). **Seismic flexural behavior of CFRP strengthened reinforced concrete beams secured with fiber anchors**. Engineering Structures, 305, 117728. https://doi.org/10.1016/j.engstruct.2024.117728

6- Yu, J., Xu, W., Yu, Y., Fu, F., Wang, H., Xu, S., Wu, S. (2022). **Cfrp strengthening and rehabilitation of inner corroded steel pipelines under external pressure**. Journal of Marine Science and Engineering, 10(5), 589. https://doi.org/10.3390/jmse10050589

7- Mokhtari, M., Nia, A. A. (2016). **The application of CFRP to strengthen buried steel pipelines against subsurface explosion**. Soil Dynamics and Earthquake Engineering, 87, 52-62. https://doi.org/10.1016/j.soildyn.2016.05.006

8- Geers, T. L., Hunter, K. S. (2002). **An integrated wave-effects model for an underwater explosion bubble**. The Journal of the Acoustical Society of America, 111(4), 1584-1601. https://doi.org/10.1121/1.1458027

9- Montazeri, E., Kazemi, S. M., Askariani, S. S. (2021). **Finite element parametric study on the cyclic response of steel frames equipped with comb-teeth dampers**. Structures, 31, 111-126. https://doi.org/10.1016/j.istruc.2021.01.033

10- Dereli, O., Basu, S., Ozbey, M., Bhattacharyya, R. (2022). **Finite element analysis of piping system under blast load due to accidental explosion**. Pressure Vessels and Piping Conference, 86168. https://doi.org/10.1115/PVP2022-86168

11- Emamzadeh, S. S. (2022). **Nonlinear dynamic response of a fixed offshore platform subjected to underwater explosion at different distances**. Journal of Marine Science and Application, 21(4), 168-176. https://doi.org/10.1007/s11804-022-00271-x

12- George, J. M., Kimiaei, M., Elchalakani, M., Fawzia, S. (2021). **Experimental and numerical investigation of underwater composite repair with fibre reinforced polymers in corroded tubular offshore structural members under concentric and eccentric axial loads**. Engineering Structures, 227, 111402. https://doi.org/10.1016/j.engstruct.2020.111402

13- Hsu, C. Y., Chiang, C. C., Luo, G. M., Chen, Y. H., Chu, F. C. (2024). **Analysis of Ship Structure with GFRP Lamination Design Subjected to Underwater Shock Loading**. Advances in Science and Technology, 136, 23-29. https://doi.org/10.4028/p-781y21

14- Liu, Z., Gudmestad, O. T., Igland, R. (2022). **Numerical Simulation of a Subsea Pipeline Subjected to Underwater Explosion Loads With the Coupled Eulerian–Lagrangian Method**. Journal of Offshore Mechanics and Arctic Engineering, 144(6), 061901. https://doi.org/10.1115/1.4054593

15- Kristoffersen, M., Hauge, K. O., Børvik, T. (2018). **Blast loading of concrete pipes using C-4 charges**. Proceedings, 60(1). https://doi.org/10.3390/proceedings2018020060

16- Lam, K., Zong, Z., Wang, Q. (2003). **Dynamic response of a laminated pipeline on the seabed subjected to underwater shock**. Composites Part B: Engineering, 34(1), 59-66. https://doi.org/10.1016/S1359-8368(02)00078-4

17- Liang, C.-C., Tai, Y.-S. (2006). **Shock responses of a surface ship subjected to noncontact underwater explosions**. Ocean Engineering, 33(5-6), 748-772. https://doi.org/10.1016/j.oceaneng.2005.05.011

18- Liu, W., Ming, F., Zhang, A., Miao, X., Liu, Y. (2018). **Continuous simulation of the whole process of underwater explosion based on Eulerian finite element approach**. Applied Ocean Research, 80, 125-135. https://doi.org/10.1016/j.apor.2018.08.015

19- Peng, Y.-X., Zhang, A.-M., Ming, F.-R. (2021). **Numerical simulation of structural damage subjected to the near-field underwater explosion based on SPH and RKPM**. Ocean Engineering, 222, 108576. https://doi.org/10.1016/j.oceaneng.2021.108576

20- Qu, Y., Wu, J., Xu, B., Li, Q. (2022). **Evaluating the shape and orientation effect of non-spherical charge on the pressure distribution of underwater explosion: Finite element analysis**. Ocean Engineering, 266, 113209. https://doi.org/10.1016/j.oceaneng.2022.113209

21- Razic, F., Miralem, B. (2019). **Underwater explosion effects of 60 mm HE mortar bomb on a cylindrical concrete structure-PIT**. Defence Technology, 15(1), 65-71. https://doi.org/10.1016/j.dt.2018.07.009

22- Tran, P., Wu, C., Saleh, M., Neto, L. B., Nguyen-Xuan, H., Ferreira, A. (2021). **Composite structures subjected to underwater explosive loadings: A comprehensive review**. Composite Structures, 263, 113684. https://doi.org/10.1016/j.compstruct.2021.113684

23- Li, S., van der Meer, D., Zhang, A.-M., Prosperetti, A., Lohse, D. (2020). **Modelling large scale airgun-bubble dynamics with highly*

[Downloaded from ijmt.ir on 2026-10-24]

non-spherical features. International Journal of Multiphase Flow, 122, 103143. https://doi.org/10.1016/j.ijmultiphaseflow.2019.103143

24- Zhang, A.-M., Li, S.-M., Cui, P., Li, S., Liu, Y.-L. (2023). **Theoretical study on bubble dynamics under hybrid-boundary and multi-bubble conditions using the unified equation*. Science China Physics, Mechanics Astronomy, 66(12), 124711. https://doi.org/10.1007/s11433-023-2216-1

25- Liang, X.-X., Linz, N., Freidank, S., Paltauf, G., Vogel, A. (2022). **Comprehensive analysis of spherical bubble oscillations and shock wave emission in laser-induced cavitation*. Journal of Fluid Mechanics, 940, A5. https://doi.org/10.1017/jfm.2022.257

26- Zhang, A.-M., Li, S.-M., Xu, R.-Z., Pei, S.-C., Li, S., Liu, Y.-L. (2024). **A theoretical model for compressible bubble dynamics considering phase transition and migration*. Journal of Fluid Mechanics, 999, A58. https://doi.org/10.1017/jfm.2024.783

27- Preso, D. B., Fuster, D., Sieber, A. B., Obreschkow, D., Farhat, M. (2024). **Vapor compression and energy dissipation in a collapsing laser-induced bubble*. Physics of Fluids, 36(3). https://doi.org/10.1063/5.0194883

28- Holian, B. L. (1988). **Modeling shock-wave deformation via molecular dynamics*. Physical Review A, 37(7), 2562. https://doi.org/10.1103/PhysRevA.37.2562

29- Kingery, C. N., Bulmash, G. (1984). **Airblast parameters from TNT spherical air burst and hemispherical surface burst*. US Army Armament and Development Center. [DOI: N/A]

30- Keller, J. B., Miksis, M. (1980). **Bubble oscillations of large amplitude*. The Journal of the Acoustical Society of America, 68(2), 628-633. https://doi.org/10.1121/1.384720

31- Taylor, G. I. (1950). **The formation of a blast wave by a very intense explosion.-II. The atomic explosion of 1945*. Proceedings of the Royal Society of London. Series A, 201(1065), 175-186. https://doi.org/10.1098/rspa.1950.0050

32- Jen, C. (2009). **Coupled acoustic–structural response of optimized ring-stiffened hull for scaled down submerged vehicle subject to underwater explosion*. Theoretical and Applied Fracture Mechanics, 52(2), 96-110. https://doi.org/10.1016/j.tafmec.2009.08.005

33- Zhou, H., Kong, X., Wang, Y., Zheng, C., Pei, Z., Wu, W. (2021). **Dynamic response of hull girder subjected to combined underwater explosion and wave induced load*. Ocean Engineering, 235, 109436. https://doi.org/10.1016/j.oceaneng.2021.109436

34- Li, L., Sun, L., Wang, T., Kang, N., Cao, W. (2019). **Repeated low-velocity impact response and damage mechanism of glass fiber aluminium laminates*. Aerospace Science and Technology, 84, 995-1010. https://doi.org/10.1016/j.ast.2018.10.026

[Downloaded from ijmt.ir on 2026-10-24]